DETUNING ESTIMATION FOR A DOUBLY-FED NORMAL-CONDUCTING GUN

M. Herrmann*, J. Branlard, F. Brinker, M. Hoffmann, V. Katalev, S. Pfeiffer, H. Schlarb, C. Schmidt
Deutsches Elektronen-Synchrotron DESY, Hamburg, Germany

Abstract

At the European Free-Electron Laser (EuXFEL) superconducting linac, a revised normal-conducting gun design with symmetrical feed was successfully installed and tested. Thermal expansion of the solid copper body dominantly affects the detuning transients of this cavity. To improve accuracy, and add time resolution over the duration of a pulse, we implemented and tested an observer that estimates the resonance frequency over time using a parameter-identified white-box model of the RF network. Results were validated against forward and reflected power couplers, cavity voltage, and an algebraic stationary approximation.

INTRODUCTION

On November 2025, a revised gun design [1] has been installed at the EuXFEL (see Fig. 1). From an RF perspective, the main changes in the current revision 5.2 are

- change from single-feed to double-feed with the individual waveguide branches equipped with forward and reflective directional couplers, and
- adding of a (redundant) cavity probe antenna.

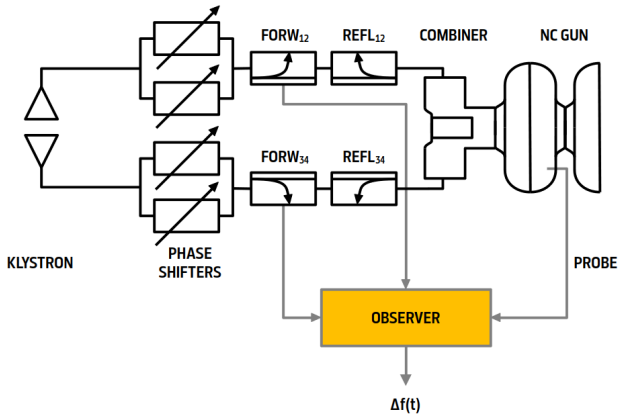

Figure 1: Gun detuning estimation scheme. The observer is a simulation of the gun running in parallel on either a CPU, or an FPGA. The observer is fed by forward voltages of the two respective branches, and the pick-up of the cavity. It serves as a virtual sensor for the unmeasurable detuning Δf.

One of the challenges operating the gun is to keep it on resonance over the course of a pulse where the intra-pulse dynamics are dominated by introduced RF energy, and interpulse dynamics are dominated by convective heat flux to the cooling medium, with the dominating source of detuning being the heat-up of the cavity's inner surface, governing a temperature-to-detuning sensitivity of approx. −21 kHz/K [2].

Since the surface temperature cannot be measured directly, we employ an observer, implemented as an Unscented Kalman filter, which can be considered a virtual (or software) sensor, to estimate time-resolved readings over the length of a pulse, representative for the unmeasurable quantity.

Assuming the estimated surface temperature to be linearly related to detuning, the observer allows for intra-pulse resolved readings of detuning, which potentially enables intra-pulse control actions.

Being an inherently model-based approach, the observer's performance depends on the accuracy of the model, triggering the need for identifying unknown system parameters.

This publication is structured as follows: the modeling section details the ordinary differential equations (odes) representing the coupled RF/detuning dynamics, section parameter identification explains the white-box parameter identification approach, and the observer section gives an outline of the implemented Kalman filter. The paper concludes with a comparison of estimated detuning and its phase-roll approximation, and an outlook for further investigations.

MODEL

By design, the Unscented Kalman filter requires a discrete-time model of the underlying dynamics that propagates the system's states from one sample to the next. In the following, this state transition map is derived from the continuous time description which, in turn, is based on first-order principles.

Continuous Time

Essentially, the gun model consists of a nonlinear 3rd-order odes for coupled RF/detuning of a normal-conducting cavity [3], plus algebraic terms for the lossless combiner [4, 5] with an additional complex parameter ε to account for asymmetry, as detailed in Eqs. (1 – 4).

$$\dot{x} = -\lambda x - yz + bu_x, \tag{1}$$
$$\dot{y} = -\lambda y + xz + bu_y, \tag{2}$$
$$\dot{z} = \rho(z - z_0) + \mu(x^2 + y^2), \tag{3}$$
$$0 = S(\varepsilon)a - a', \tag{4}$$

where x and y are real and imaginary voltage, z is detuning, $b = \frac{2\beta}{\beta+1}\lambda$ is input scalar, λ is half bandwidth, u_x and u_y are real and imaginary forward voltage, z_0 is initial detuning, β

* m.herrmann@desy.de

is coupling factor,

$$S(\varepsilon) = \begin{pmatrix} -j/2 & j/2 & \frac{1}{\sqrt{2}}\varepsilon \\ j/2 & -j/2 & \frac{1}{\sqrt{2}} \\ \frac{1}{\sqrt{2}}\varepsilon & \frac{1}{\sqrt{2}} & 0 \end{pmatrix} \tag{5}$$

is the combiner's scattering matrix at 1.3 GHz, $a = (V_{\text{forw},12}, V_{\text{forw},34}, u)$ and $a' = (V_{\text{refl},12}, V_{\text{refl},34}, V_{\text{refl}})$ are complex-valued inputs and outputs of the combiner, respectively, and ρ and μ are temperature-to-detuning and RF-to-detuning sensitivity, respectively. Finally, $\varepsilon = |\varepsilon|e^{i\angle\varepsilon}$ is a complex calibration coefficient accounting for the combiner's asymmetry.

For the discrete-time description of the above given model, we exploit its integrability property [6], observing that the dynamics associated to convective cooling are considerably slower than energy intake due to RF, rendering the first term in the detuning transient negligible over the length of a pulse ($\rho \ll \mu$). We then introduce a change from Cartesian to polar coordinates

$$x = r\cos(\theta), \tag{6}$$
$$y = r\sin(\theta), \tag{7}$$

which transforms Eq. (1 – 3) into

$$\dot{r}\cos(\theta) - r\dot{\theta}\sin(\theta) = -\lambda r\cos(\theta) - r\sin(\theta)z + u_x, \tag{8}$$
$$\dot{r}\sin(\theta) + r\dot{\theta}\cos(\theta) = -\lambda r\sin(\theta) + r\cos(\theta)z + u_y, \tag{9}$$
$$\dot{z} = \mu r^2. \tag{10}$$

Rotating the input signals

$$\begin{pmatrix} u_x \\ u_y \end{pmatrix} = \underbrace{\begin{pmatrix} \cos(\theta) & -\sin(\theta) \\ \sin(\theta) & \cos(\theta) \end{pmatrix}}_{R(\theta)} \begin{pmatrix} u_r \\ u_\theta \end{pmatrix}, \tag{11}$$

and doing the transform (1) $\cos(\theta)$ + (2) $\sin(\theta)$ reduces the time evolution of the amplitude to a nonautonomous linear ode in r:

$$\dot{r} = -\lambda r + u_r, \tag{12}$$

or, equivalently, its convolution

$$r(t) = r_0 e^{-\lambda t} + \int_0^t e^{-\lambda(t-\tau)} u_r(\tau) d\tau. \tag{13}$$

Now that the amplitude r is given explicitly as an expression of time, detuning z is obtained by a straight-forward integration

$$z(t) = z_0 + \mu \int_0^t r^2(\tau) d\tau. \tag{14}$$

In a similar fashion, transforming -(1) $\sin(\theta)$ + (2) $\cos(\theta)$ yields the forced transients for the phase θ

$$r\dot{\theta} = rz + u_\theta \quad \underleftrightarrow{r \neq 0} \quad \dot{\theta} = z + u_\theta / r, \tag{15}$$

which, again, can be integrated directly using the functions $z(t)$, and $r(t)$:

$$\theta(t) = \theta_0 + \int_0^t z(\tau) + u(\tau)/r(\tau) d\tau. \tag{16}$$

Discrete Time

Integrating (13), (14), and (16) over the limits of two successive time points $t_{k+1} - t_k = T_s$, where T_s is sample time, employing a symbolic solver [7], and assuming zero-order hold behavior for the inputs u_r, u_θ, eventually yields the desired state transition map

$$\eta_{k+1} = f(\eta_k, v_k). \tag{17}$$

The right-hand side of the mapping (17) is a lengthy, vector-valued expression in its arguments $\eta_k = (r_k, \theta_k, z_k)$, $v_k = (u_{r,k}, u_{\theta,k})$.

The full procedure for computing the next time step is as follows:

1. Choose previous state η_k and input u_k.
2. Compute input $v_k = R(\theta_k)^{-1} u_k$.
3. Compute next time step[1] $\eta_{k+1} = f(\eta_k, v_k)$.

The obvious advantage of this method is its favorable trade-off of computational cost vs accuracy: an Euler-forward scheme for integrating the set of odes (1) to (3) diverges within a couple of time steps, i.e. introduces numerical instabilities if time steps are chosen too large, whereas a numeric quadrature is accurate, but infeasible for implementation on FPGA.

PARAMETER IDENTIFICATION

Departing from manually tuned system parameters and calibration coefficients that made for the initial matching of measurements and simulations, the parameters have been refined by applying a direct-search optimization scheme[2] on the subset of pulse samples that exhibit dynamics, with the cost function defined as

$$J(x) = \sum_k |y_{\text{sim},k}(x) - y_{\text{meas},k}|^2, \tag{18}$$

where $x = (\varepsilon, a_{12}, a_{34}, \beta, z_0)$ are the decision variables, i.e. the system parameters (β, z_0) and calibration coefficients[3] (a_{12}, a_{34}) to be identified, and $y = (y_{\text{probe}}, y_{\text{forw}}, y_{\text{refl}})$ denotes measurements.

The RF-to-detuning parameter μ was excluded from the parameter estimation, and determined from prior simulation results [8] by integrating Eq. (3):

$$\Delta\omega = \mu \int_0^T E_c^2 = K_f P_{\text{ref}} \left(\frac{E_c}{E_{c,\text{ref}}} \right)^2 T, \tag{19}$$

where E_c is constant pulse gradient, T is pulse length, and the remaining parameters are tabulated values given in [8].

[1] Note that the corner case $r = 0$ needs special attention, since Eq. (15) is undefined for vanishing amplitude.

[2] We used a Nelder-Mead algorithm, since gradient-based methods apparently had difficulties leaving the vicinity of the initial guess.

[3] For scaling and rotating the forward voltage signal

OBSERVER

Since the free dynamics η of the transformed system (10), (12), (15) can be explicitly expressed as a function of measurements (r, θ), and their time derivatives,

$$\eta = (r, \theta, \dot{\theta}), \tag{20}$$

the system (1) to (4) is, apart from $r = 0$, globally observable [9], and thereby qualifies as a candidate for estimation schemes. An instance [10] of the Unscented Kalman filter [11] estimates the unmeasurable detuning. It was chosen for ease of implementation, for its robustness, and applicability to nonlinear systems. The key feature that distinguishes the Unscented Kalman filter from other implementations is that the (nonlinear) state transition map f is applied to a set of $N_\Sigma = 3$ sampled states η to compute the error covariance matrix for the next time step, i.e. for every time step, N_Σ evaluations of f are required. The parameters that define the filter are sigma points, the covariance matrices, and the choice of initial condition, and are discussed in the following.

Covariance Matrices

To account for process noise Q, measurement noise R, and initial state error P_0, the respective covariance matrices are structured as follows:

$$Q = \begin{pmatrix} q^2 & 0 & 0 \\ 0 & q^2 & 0 \\ 0 & 0 & 0 \end{pmatrix}, \qquad R = r^2 I_2, \qquad P_0 = I_3 \tag{21}$$

with $q = 0.02$ accounting for quantization noise, and $r = 10^{-3}$ chosen conservatively as measurement noise.

Initial State

The better the choice of the initial state η_0, the better the estimation of the detuning. For the time being, we are dealing with pulsed operation exclusively, s.t. the initial values for amplitude and phase are $r_0 = \theta_0 = 0$. Initial detuning z_0 mainly depends on cooling water temperature, flow rate, and the time between two consecutive pulses. One could model the heat-flux related drop in detuning online by letting the observer run continuously with the convective term in Eq. (3) enabled, i.e. $\rho \neq 0$. We have decided to have the observer run in pulsed mode instead, and make use of one of the fundamental properties of an observable system, namely the capability of reconstructing the initial state from a set of current measurements which is then used as an initial guess for the next pulse.

Similar to the parameter identification, we employ a direct-search optimization scheme

$$\min_{x_0} \sum_k |y_{\text{meas},k} - C f^k(x_0, u_k)|^2, \tag{22}$$

where x_0 are the initial conditions, and $C = [I_2, 0]$ is the measurement matrix.

RESULTS

The observer was run on a CPU as a batch process, updating the detuning trace with approx. 3 Hz. We compared the computed detuning at the end of the pulse with a stationary approximation of the detuning. The results are shown in Fig. 2 over the duration of one day ($N \approx 10^5$), which indicates a considerable reduction of measurement noise for the same mean value.

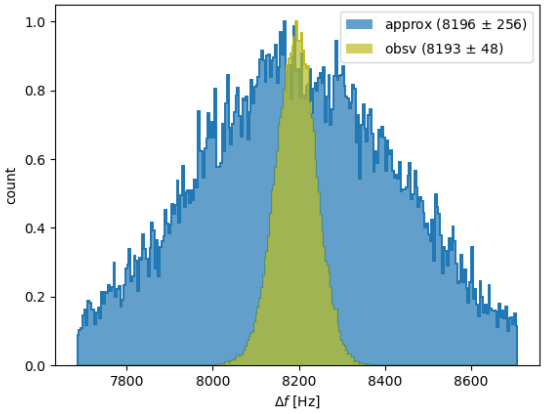

Figure 2: Estimated detuning at the end of the pulse. The histogram shows a comparison of the detuning computation using a phase roll approximation (*blue*) vs. the estimated detuning obtained from the observer (*green*). The spread of the Kalman filter is by a factor 5 smaller.

CONCLUSION

We have shown that an Unscented Kalman filter combined with initial state recovery based on a nonlinear cavity model can effectively reduce the detuning measurement noise of a normal-conducting gun in pulsed mode, opening up new performance potentials for enhanced control laws. By design not limited to pulsed mode and gun cavities, the algorithm could equally be deployed on FPGA and super-conducting structures, enabling online estimation and CW-readiness.

ACKNOWLEDGEMENTS

This work was partially funded in the context of the R&D program of the European XFEL. This project has also received funding from the European Unions Horizon Europe research and innovation program under grant agreement N. 101131435

REFERENCES

[1] A. Oppelt *et al.*, "Status of the L-band gun development at PITZ", in *Proc. LINAC2024*, Chicago, IL, USA, pp. 317–319, Aug. 2024. doi:10.18429/JACoW-LINAC2024-TUAA012

[2] S. Pfeiffer *et al.*, "Precision feedback control of a normal conducting standing wave resonator cavity", *Phys. Rev. Accel. Beams*, vol. 21, no. 9, p. 092802, Sep. 2018. doi:10.1103/PhysRevAccelBeams.21.092802

[3] T. Schilcher, "Vector sum control of pulsed accelerating fields in Lorentz force detuned superconducting cavities", Ph.D. thesis, DESY, Hamburg, Germany, 1998.

[4] V. Katalev, "LLRF measurements of S coupler for Gun 5", DESY, Hamburg, Germany, Rep. unpublished, Jun. 2023.

[5] A. Morini, T. Rozzi, M. Farina, and P. Angeletti, "Scattering matrix of a reciprocal, lossless, and symmetrical three-port power divider", *IEEE Microw. Wirel. Technol. Lett.*, vol. 33, no. 2, pp. 130–132, 2023. doi:10.1109/LMWC.2022.3216023

[6] M. Herrmann and Goncalo, "Integrability of a system with quadratic nonlinearities", Mathematics Stack Exchange, Question 5133079, Version: 2026-04-16, 2026, https://math.stackexchange.com/questions/5133079/,

[7] A. Meurer *et al.*, "SymPy: symbolic computing in Python", *PeerJ Comput. Sci.*, vol. 3, e103, Jan. 2017. doi:10.7717/peerj-cs.103

[8] N. Brusova, V. Paramonov, I. Rybakov, and A. Skasyrskaya, "Physical specifications of the Gun 5 RF cavity for X-FEL requirements", in *Proc. 60th October Anniversary Prospect*, Moscow, Russian Federation, 2016, pp. 1–68.

[9] M. Zeitz, "Observability canonical (phase-variable) form for non-linear time-variable systems", *Int. J. Syst. Sci.*, vol. 15, no. 9, pp. 949–958, 1984. doi:10.1080/00207728408926614

[10] R. Labbe, KALMAN-AND-BAYESIAN-FILTERS-IN-PYTHON, GitHub, Oct. 2020. https://github.com/rlabbe/Kalman-and-Bayesian-Filters-in-Python

[11] S. J. Julier and J. K. Uhlmann, "New extension of the Kalman filter to nonlinear systems", in *Proc. AeroSense '97, Signal Processing, Sensor Fusion, and Target Recognition VI*, Orlando, FL, USA, vol. 3068, pp. 182–193, 1997. doi:10.1117/12.280797